

Many-Body Approximation Scheme Beyond GW

Ping Sun¹ and Gabriel Kotliar¹

¹*Department of Physics and Astronomy, Rutgers University, Piscataway, NJ 08854-8019*

(Dated: November 23, 2018)

We explore the combination of the extended dynamical mean field theory (EDMFT) with the GW approximation (GWA); the former sums the local contributions to the self-energies to infinite order in closed form and the latter handles the non-local ones to lowest order. We investigate the different levels of self-consistency that can be implemented within this method by comparing to the exact QMC solution of a finite-size model Hamiltonian. We find that using the EDMFT solution for the local self-energies as input to the GWA for the non-local self-energies gives the best result.

PACS numbers: 71.10.-w, 71.27.+a

Introduction.– The GW approximation (GWA) [1] is one of the most successful methods to describe electronic structure of weakly correlated materials. It includes the lowest order perturbative corrections in the screened Coulomb interaction to the electron self-energy. In real space-time, the electron self-energy is given by the product “GW”, where “G” represents the electron Green’s function and “W” the RPA screened Coulomb interaction. The GWA has been successfully applied to the calculations of quasi-particle spectra of semiconductors and insulators. [2] (For recent reviews, see Ref.[3]) It describes well the experimentally observed energy gaps in semiconductors [3, 4, 5, 6, 7, 8].

The GWA self-energies were first calculated as a one-shot perturbation by using the unperturbed LDA Green’s functions. [2] However, as we will show in this paper, the one-shot GWA breaks down as soon as the correlations are moderately strong, as expected for a non-self-consistent leading order approximation. The problem should be solved by including higher order corrections to extend the scope of the method. This is the main motivation of our work. The Baym-Kadanoff formulation [9] of the GWA, which makes the method automatically conserving, requires to evaluate the self-energy, the polarization bubble, and the Green’s function self-consistently [1]. While this has been successfully implemented [10] and shows improvement on the values of the total energy, the self-consistent GWA brings up a debate over whether the fully self-consistency improves the spectra. [6, 7, 8, 11, 12, 13, 14]. This is due to the fact that the vertex correction, which is omitted in GWA, shows a tendency to cancel the self-energy insertion when the full Green’s function is used in calculating the exchange self-energy [15, 16, 17]. As a result the one-shot GWA or partial-self-consistent ones (in which, *e.g.*, one fixes the “W” obtained from the LDA input while solving “G” self-consistently) are favored sometimes [11, 12, 13]. This issue entails the usage of higher order self-energy diagrams and provides us a second motivation for improving systematically the approximation beyond the leading order.

In this paper, we extend the GWA by using the extended dynamical mean field theory (EDMFT) [18, 19, 20, 21] which treats all the local polarization, self-energy

and vertex corrections in closed form, following the ideas proposed in Refs.[20, 21, 22]. According to these approaches, the local polarization and self-energy should be solved by EDMFT non-perturbatively while the non-local ones via GWA. The cancellation of the self-energy insertion and the vertex correction is carried out *locally* to infinite order within EDMFT. However, the same ambiguity of implementation (with or without self-consistency) remains in the non-local GWA part. This question can not be addressed without benchmarking the different schemes.

Main Results.– We compared and contrasted the different implementations of combining EDMFT with GWA. Our numerical calculation suggests that the schemes using the EDMFT solution of the local self-energies as input to the GWA for the non-local self-energies give the best result. In other words, it is favorable *not* to allow the feedback of the non-local GWA on the local EDMFT self-energies due to different nature of the two methods, GWA being perturbative and EDMFT non-perturbative. On the other hand, when using the EDMFT result as input, it makes little difference whether one performs GWA with a single shot or partial self-consistency (it is partial because the local polarization and self-energy from EDMFT are fixed). This supports the picture [21, 22] that, in a correlated phase far away from a phase transition, the temporal correlations reflected through the local polarization and self-energy are dominant and should be treated non-perturbatively, while the spatial correlations are weaker and can be handled perturbatively.

Lattice Model.– In comparing different GW approaches, many of which apply to realistic materials, one always encounters the problem that there are as many important differences in the implementations as in the GWA methodologies themselves. These include the implementations of GWA in imaginary time or frequency space, the choice and construction of the local basis set, and the further approximations like the plasmon-pole approximation [3]. In order to compare the many-body schemes without additional complications, it is desired to employ simple model systems on the lattice [11, 23]. Following the same strategy, we study the following generalized Hubbard model:

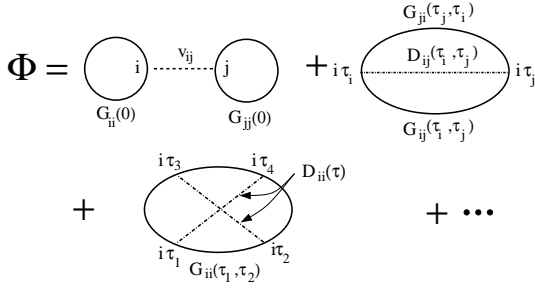


FIG. 1: The potential Φ of the Baym-Kadanoff functional [9, 19] for $(\text{EDMFT}+\text{GW})_{SC}$. $(\text{EDMFT})_{SC}$ is obtained by restricting the exchange diagram (the second on the r.h.s.) to be local in space, $i = j$. The first line by itself represents the standard $(\text{GW})_{SC}$ scheme. In this formulation, the boson Green's function D describes the screened interaction. The boson self-energy plays a similar role as the electron-hole bubble in GWA.

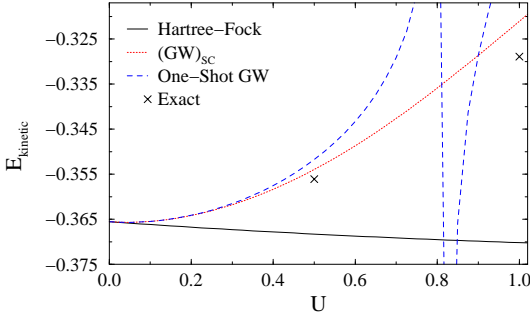


FIG. 2: In our model system, the one-shot GWA, using the Hartree-Fock result as input, breaks down at $U \simeq 0.825$. This is an instability against the formation of charge density wave at (π, π) [27]. The other results are plotted as references.

$$\hat{H} = -\frac{1}{2} \sum_{ij, \sigma} t_{ij} (\hat{c}_{i\sigma}^\dagger \hat{c}_{j\sigma} + \hat{c}_{j\sigma}^\dagger \hat{c}_{i\sigma}) + \frac{1}{2} \sum_{ij} \hat{n}_i v_{ij} \hat{n}_j \quad (1)$$

where $\hat{c}_{i\sigma}$ ($\hat{c}_{i\sigma}^\dagger$) annihilates (creates) an electron of spin σ ($=\uparrow, \downarrow$) at the lattice site i . \hat{n}_i is the electron density. We only consider the paramagnetic phase.

Approximation Schemes.— The self-consistent schemes are summarized in Fig.1. [we use $(\dots)_{SC}$ for a self-consistent (SC) loop and $(\dots)_{PSC}$ a partially SC loop.] The full functional in Fig.1 can be separated into local and non-local parts, which are functionals of the local and non-local Green's functions, respectively: $\Phi = \Phi_{EDMFT}[G_{Local}, D_{Local}] + \Phi_{Non-Local GW}[G_{Non-Local}, D_{Non-Local}]$. The local (non-local) self-energies, which are obtained from the functional derivatives of Φ_{EDMFT} ($\Phi_{Non-Local GW}$), are functions of the local (non-local) parts of the Green's functions only: $\Sigma_{EDMFT} = \Sigma_{EDMFT}(G_{Local}, D_{Local})$ and $\Sigma_{Non-Local GW} = \Sigma_{Non-Local GW}(G_{Non-Local}, D_{Non-Local})$ for the electron, $\Pi_{EDMFT} = \Pi_{EDMFT}(G_{Local}, D_{Local})$ and

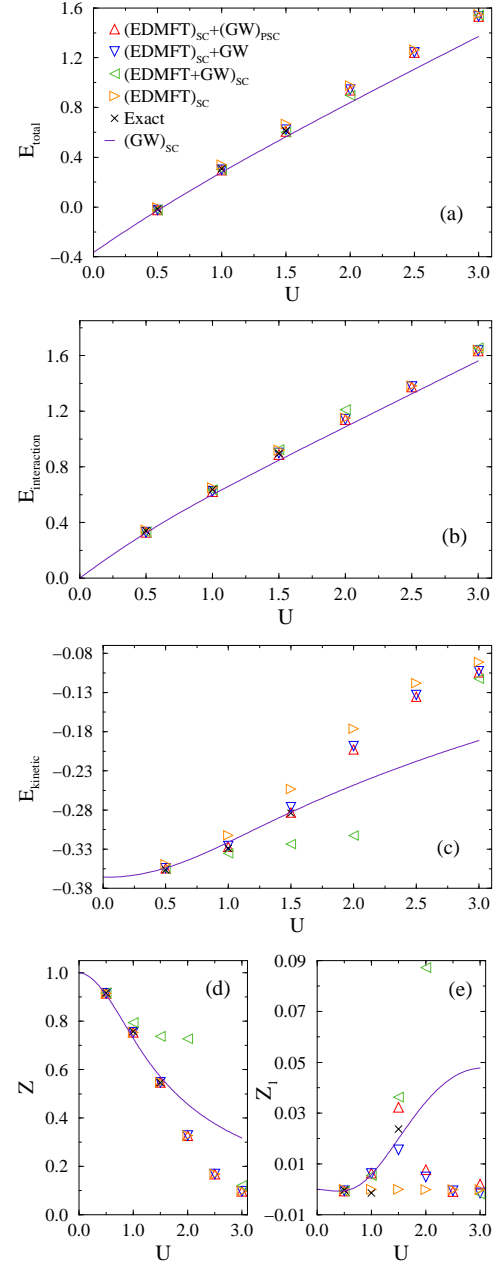


FIG. 3: The energies, the quasi-particle residue (Z), and the non-local contribution to the self-energy (Z_1) as defined in the text. The same symbol scheme defined in (a) applies to all the diagrams. Z is the same for $(\text{EDMFT})_{SC}+(\text{GW})_{PSC}$, $(\text{EDMFT})_{SC}+\text{GW}$, and $(\text{EDMFT})_{SC}$, since the same local self-energy is used. For Z_1 , which reflects the spatial extension of the self-energy, we are comparing numbers at least one order smaller than those for other quantities.

$\Pi_{Non-Local GW} = \Pi_{Non-Local GW}(G_{Non-Local})$ for the boson.

The approximation schemes we tested in combining EDMFT with GW are: (i) The fully self-consistent $(\text{EDMFT}+\text{GW})_{SC}$ solves the full Dyson equations for $G = G_{Local} + G_{Non-Local}$ and $D = D_{Local} + D_{Non-Local}$:

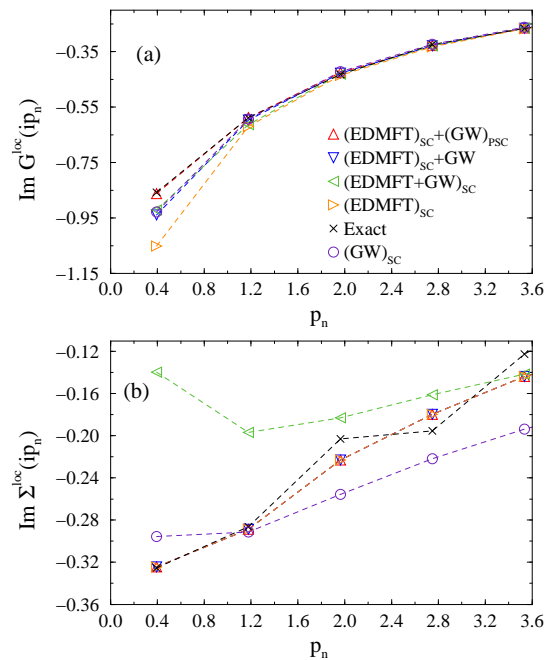


FIG. 4: The local electron Green's function and self-energy at $U = 1.5$. The same symbol scheme defined in (a) applies to (b). The lines connecting the points are guides to the eye. The fermion Matsubara frequency $p_n = (\pi/\beta)(2n + 1)$.

$G = [G_0^{-1} - \Sigma_{EDMFT} - \Sigma_{Non-Local GW}]^{-1}$,
 $D = [D_0^{-1} - \Pi_{EDMFT} - \Pi_{Non-Local GW}]^{-1}$, with
 G_0 and D_0 the free electron and boson Green's
functions on the lattice. The non-self-consistent
schemes begin with the solution of the EDMFT
which solves $G_{Local} = [G_0^{-1} - \Sigma_{EDMFT}]_{Local}^{-1}$
and $D_{Local} = [D_0^{-1} - \Pi_{EDMFT}]_{Local}^{-1}$. (ii)
(EDMFT) $_{SC}+GW$ uses the local EDMFT self-
energies to calculate the non-local Green's functions,
 $G_{EDMFT,Non-Local} = [G_0^{-1} - \Sigma_{EDMFT}]_{Non-Local}^{-1}$ and
 $D_{EDMFT,Non-Local} = [D_0^{-1} - \Pi_{EDMFT}]_{Non-Local}^{-1}$. It
obtains in one shot the estimation for $\Sigma_{Non-Local GW} =$
 $\Sigma_{Non-Local GW}(G_{EDMFT,Non-Local}, D_{EDMFT,Non-Local})$
and $\Pi_{Non-Local GW} = \Pi_{Non-Local GW}(G_{EDMFT,Non-Local})$. (iii)
(EDMFT) $_{SC}+(GW)_{PSC}$ solves for $G_{Non-Local}$ and
 $D_{Non-Local}$ self-consistently from $G_{Non-Local} = [G_0^{-1} -$
 $\Sigma_{EDMFT} - \Sigma_{Non-Local GW}]_{Non-Local}^{-1}$ and $D_{Non-Local} =$
 $[D_0^{-1} - \Pi_{EDMFT} - \Pi_{Non-Local GW}]_{Non-Local}^{-1}$ with
 Σ_{EDMFT} and Π_{EDMFT} fixed.

Benchmark.— To compare and contrast the approxima-
tion schemes, we perform a benchmark calculation using
the model (1) on a 4×4 , 2D square lattice with peri-
odic boundary condition. We use, for the free electron
dispersion, $\epsilon_{\vec{k}} = -(1/2)[\cos(k_x) + \cos(k_y)]$. The half-
bandwidth is taken as the energy unity. The interac-
tion is given by $v_{\vec{k}} = U + 2V[\cos(k_x) + \cos(k_y)]$. We
study the half-filling case where the strongest correlation
shows up. We fix the inverse temperature $\beta = 8.0$ and

the ratio $V/U = 0.25$. We vary U from 0.0 to 3.0 for
the approximation schemes. We benchmark the calcula-
tion at $U = 0.5, 1.0, 1.5$ by using direct QMC calcula-
tion via the Hirsch-Fye algorithm [24]. In all the results we
are going to present, the major error of the calculation
comes from the QMC part, in both the exact solution
and the EDMFT impurity solver. In the latter we solve
the EDMFT electron-boson impurity problem by a hy-
bridized Monte Carlo method [21, 25, 26, 27] which em-
ploys an additional continuous auxiliary field. [28]

At the given V-U ratio, a charge density wave instabil-
ity at wave vector (π, π) is present in the one-shot GW.
The breakdown is shown in Fig. 2. In the exact solu-
tion, however, no charge or spin instability is observed
up to $U = 1.5$. To compare the different schemes on
the same footing, we restrict ourselves to the paramag-
netic phase. Depending on the different schemes, this
may mean to studying a paramagnetic metastable solu-
tion when the possible instability appears. We find it al-
lowed for (GW) $_{SC}$ up to the largest $U (= 3.0)$ we studied
and same for the EDMFT related schemes we described,
except for (EDMFT+GW) $_{SC}$ in which the self-consistent
solution does not exist at $U = 2.5$.

Our main results are presented in Figs. 3 and 4
in which the results from the exact QMC and the
(GW) $_{SC}$ are also plotted. The definitions of the
plotted quantities are as follows: The $E_{kinetic}$ and
 $E_{interaction}$ are the hopping and interaction energies
per site, calculated via the Galitskii-Migdal formula
[29]. $E_{total} = E_{kinetic} + E_{interaction}$. The local elec-
tron self-energy of (EDMFT) $_{SC}$ is obtained directly
from the EDMFT solution while for those with spa-
tial extension, $\Sigma^{loc}(ip_n) = (1/N)\sum_{\vec{k}}\Sigma(\vec{k}, ip_n)$, with
 $N = 4 \times 4$. The local Green's function $G^{loc}(ip_n) =$
 $(1/N)\sum_{\vec{k}}\{[G_0(\vec{k}, ip_n)]^{-1} - \Sigma(\vec{k}, ip_n)\}^{-1}$. The quasi-
particle residue $Z = [1 - \text{Im} \Sigma^{loc}(ip_0)/p_0]^{-1}$. We measure
the spatial extension of the electron-self-energy by $Z_1 =$
 $(1/N)\sum_{\vec{k}} \text{Im}\{[\Sigma(\vec{k}, ip_1) - \Sigma(\vec{k}, ip_0)]/(p_1 - p_0)\} \cos k_x$.

From the *overall* features of the results, we see: (i) The
(EDMFT) $_{SC}+(GW)_{PSC}$ gives the best results up to the
largest benchmarked U at 1.5 times the half-bandwidth.
(ii) The difference between (EDMFT) $_{SC}+(GW)_{PSC}$ and
(EDMFT) $_{SC}+GW$ is small quantitatively, since the lo-
cal self-energies from (EDMFT) $_{SC}$ is dominant. (iii)
(EDMFT+GW) $_{SC}$ is not a good scheme in the sense that
it sees an artificial charge density instability around $U \sim$
2.5, where no self-consistent solution is found. Even be-
fore reaching that regime, the (EDMFT+GW) $_{SC}$ shows
significant deviations from the exact solution. (iv) From
the plottings of Z and Z_1 in Fig. 3, we see that (GW) $_{SC}$
misses the crossover to localization at large U , while the
EDMFT based calculations correctly capture this fea-
ture. Actually, all the EDMFT related schemes give re-
sults close to each other at $U = 3.0$ since the spatial
extensions of the self-energies are no longer important.
Our results show that, with moderate and strong correla-
tions, one needs to include higher order contributions be-

yond GWA. The schemes, (EDMFT) $_{SC}+(GW)_{PSC}$ and (EDMFT) $_{SC}+GW$, offer a reliable solution towards this direction.

Conclusion.— To summarize, we presented a many-body scheme which handles the local self-energies non-perturbatively via EDMFT and the non-local ones perturbatively via GWA. As an improvement over the leading order GWA, the new scheme better captures the effects of correlation. We described several implementations, which perform self-consistency at different levels, and benchmarked them by comparing with the exact solution of a finite-size model system. We found that (EDMFT) $_{SC}+(GW)_{PSC}$ and (EDMFT) $_{SC}+GW$ gave very close results. For the model we studied, (EDMFT) $_{SC}+(GW)_{PSC}$ gave the best result.

Finally, we should point out that, similar to the self-

consistent GWA [13, 16], our scheme has the problem that the polarization does not have the proper asymptotic behavior in the long wave length limit [$\lim_{k \rightarrow 0} P(k, \omega) \propto (k/\omega)^2$]. Since the schemes combining EDMFT with GWA include local vertex corrections non-perturbatively, this violation is less severe than that in GWA. [27, 30]

Acknowledgements.— This research was supported by NSF under Grant No. DMR-0096462 and by the Center for Materials Theory at Rutgers University. The authors would like to thank A. Lichtenstein based on whose multiband QMC program part of the exact QMC calculation was performed. P.S. would like to thank the helpful discussions with H. Jeschke, W. Ku, C. Marianetti, V. Oudovenko, S. Savrasov, R. Scalettar, M. Schilfhaarde, and S. Zhang.

-
- [1] L. Hedin, Phys. Rev **139**, A796 (1965); L. Hedin and S. Lundqvist, *Solid State Physics*, eds. H. Ehrenreich, F. Seitz, and D. Turnbull Academic, New York, Vol. **23**, 1 (1969).
- [2] G. Strinati, H. J. Mattausch, and W. Hanke Phys. Rev. Lett. **45**, 290 (1980); Phys. Rev. B **25**, 2867 (1982); M. Hybertsen and S. G. Louie, Phys. Rev. B **34**, 5390 (1986); R. W. Godby, M. Schluter, and L. J. Sham, Phys. Rev. B **35**, 4170 (1987).
- [3] F. Aryasetiawan and O. Gunnarsson, Rep. Prog. Phys. **61**, 237 (1998); W. G. Aulbur, L. Jonsson, and J. W. Wilkins, *Solid State Physics*, eds. F. Seitz, D. Turnbull, and H. Ehrenreich, Academic, New York, vol **54**, 1 (2000).
- [4] E. L. Shirley, X. Zhu, and S. G. Louie, Phys. Rev. B **56**, 6648 (1997).
- [5] T. Kotani and M. van Schilfhaarde, Sol. State. Comm. **121**, 461 (2002).
- [6] W. Ku and A. G. Eguiluz, Phys. Rev. Lett. **89**, 126401 (2002).
- [7] M. L. Tiago, S. Ismail-Beigi, S. G. Louie, cond-mat/0307181.
- [8] S. V. Faleev, M. van Schilfhaarde, and T. Kotani, cond-mat/0310677.
- [9] G. Baym and L. P. Kadanoff, Phys. Rev. **124**, 287 (1961); G. Baym, Phys. Rev. **127**, 1391 (1962).
- [10] H. J. de Groot, P. A. Bobbert, and W. van Haeringen, Phys. Rev. B **52**, 11000 (1995); E. L. Shirley, Phys. Rev. B **54**, 7758 (1996).
- [11] F. Aryasetiawan, T. Miyake, and K. Terakura, Phys. Rev. Lett. **88**, 166401 (2002).
- [12] P. Garcia-Gonzalez and R. W. Godby, Phys. Rev. B **63**, 75112 (2001).
- [13] B. Holm and U. von Barth, Phys. Rev. B **57**, 2108 (1998).
- [14] W.-D. Schone and A. G. Eguiluz, Phys. Rev. Lett. **81**, 1662 (1998).
- [15] B. E. Sernelius, Phys. Rev. B **36**, 1080 (1987).
- [16] See the review by G. D. Mahan, Comm. Cond. Matt. Phys. **16**, 333 (1994).
- [17] B. Holm and F. Aryasetiawan, Phys. Rev. B **56**, 12825 (1997).
- [18] J. L. Smith and Q. Si, Phys. Rev. B **61**, 5184 (2000); Q. Si and J. L. Smith, Phys. Rev. Lett. **77**, 3391 (1996); H. Kajueter, Ph.D. thesis, Rutgers University (1996).
- [19] R. Chitra and G. Kotliar, Phys. Rev. B **63**, 115110 (2001).
- [20] G. Kotliar and S. Y. Savrasov, in *New Theoretical Approaches to Strongly Correlated Systems*, edited by A. M. Tsvelik (Kluwer Academic, Dordrecht, 2001).
- [21] P. Sun and G. Kotliar, Phys. Rev. B **66**, 085120 (2002).
- [22] S. Biermann, F. Aryasetiawan, and A. Georges, Phys. Rev. Lett. **90**, 086402 (2003).
- [23] C. Verdozzi, R. W. Godby, and S. Holloway, Phys. Rev. Lett. **74**, 2327 (1995); T. J. Pollehn, A. Schindlmayr, and R. W. Godby, J. Phys. Cond. Matt **10**, 1273 (1998); A. Schindlmayr, T. J. Pollehn, and R. W. Godby, Phys. Rev. B **58**, 12684 (1998).
- [24] J. E. Hirsch and R. M. Fye, Phys. Rev. Lett. **56**, 2521 (1986).
- [25] G. M. Buendia, Phys. Rev. B **33**, 3519 (1986); J. K. Freericks, M. Jarrell, and G. D. Mahan, Phys. Rev. Lett. **77**, 4588 (1996).
- [26] Y. Motome and G. Kotliar, Phys. Rev. B **62**, 12800 (2000).
- [27] P. Sun and G. Kotliar, paper in preparation.
- [28] In QMC, we use 32 time slices. For each EDMFT iteration, we perform 10^6 QMC sweeps and usually EDMFT converges after about 10 iterations. In the case of the exact solution, due to the sign problem, the effective number of QMC sweeps is reduced from the actual number $\sim 5 \times 10^4$. In the worst case at $U = 1.5$ the effective sweep number becomes $\sim 10^4$. To proceed beyond $U = 1.5$, one needs to use approximated algorithms other than the exact QMC to overcome the sign problem.
- [29] V. M. Galitskii and A. B. Migdal, Sov. Phys. JETP **7**, 96 (1958).
- [30] At $U = 1.5$, we find the polarizations $P(k = 0, i\omega_n)$ at $n = 32$ (so $\omega_n = 25.13$) are: -1.88E-3 for (GW) $_{SC}$, -4.6E-4 for (EDMFT) $_{SC}$, -1.3E-4 for (EDMFT+GW) $_{SC}$, -6E-5 for (EDMFT) $_{SC}+GW$, and 8E-5 for (EDMFT) $_{SC}+(GW)_{PSC}$. In all the cases we studied, the GWA always results in a much bigger violation than the EDMFT related methods, especially those obtained from combining EDMFT with GWA.